Received: 6 July 2019 | Revised: 13 March 2020 | Accepted: 24 April 2020

DOI: 10.1002/we.2525

WILEY

RESEARCH ARTICLE

Micrositing under practical constraints addressing the energy-noise-cost trade-off

Prateek Mittal | Kishalay Mitra

Global Optimization and Knowledge Unearthing Laboratory, Department of Chemical Engineering, Indian Institute of Technology Hyderabad, Telangana, India

Correspondence
Kishalay Mitra, Global Optimization and Knowledge Unearthing Laboratory, Department of Chemical Engineering, Indian Institute of Technology Hyderabad, Kandi, Telangana 502285, India.
Email: kishalay@iith.ac.in

Funding information
SPARC Project, Ministry of Human Resources Development, Government of India, Grant/Award Number: SPARC/2018- 2019/P1084/SL; SPARC project, Grant/Award Number: SPARC/2018-2019/P1084/SL

Peer Review
The peer review history for this article is available at https://publons.com/publon/10.1002/we.2525.

Abstract

Wind energy is running well ahead of its peers to deal with the demand–supply and environmental crisis due to fossil fuels. However, continuous exploitation of land led wind farms built in close proximity of dwellings of human beings, restricted zones, causing adverse effect on health and the environment. In this work, using a widely used model for wake and acoustic model (ISO-9613-2), the optimal number and locations of turbines in a farm has been determined while meeting several conflicting objectives such as noise propagation, energy, and cost. An index-based decomposition and repair strategy (iDRS) using different indices for grid locations and performing repair on chromosomes to enhance the performance of convergence has been proposed as solution methodology. Comparing with a well-established case study, the methodology is applied next to another realistic case, where the effects of the presence of practical constraints on the optimal layout are demonstrated. A designer can select a layout from several choices from the obtained Pareto set of solutions based on the permissible noise limits, cost obligations, and the extent of harnessed energy.

KEYWORDS
decomposition, energy, evolutionary, micrositing, multiobjective optimization, noise

1 | INTRODUCTION

The renewable sources of energy are slowly taking the center stage as the conventional sources are depleting as well as showing environmental concerns. Amidst several renewable energy options, the wind energy turns out to be the leader because of the associated attractive features such as lower operational cost, cleaner production, and easy availability.[1] The popularity is reflected through the remarkable attention wind energy has gained among researchers, industries, and federal policies.[2,3] Following the uprising trend, the Global Wind Energy Council (GWEC) has recorded ~539 GW of overall installed capacity of wind farms at the end of 2017 and predicted the same to rise by ~55% by 2022.[4] Generally, energy from wind is trapped using group of turbines placed inside a wind farm, which convert the kinetic energy of wind into electrical form of energy. However, the layout optimization (LO) of wind farm (i.e., determination of both optimum number and position of wind turbines inside a wind farm), also known as micrositing, is a challenging task. Following the myth of more energy can be generated with more number of turbines, wind farm developers often install more turbines inside wind farms causing effectively a major reduction in wind speed due to the inter turbine wake effects leading to overall reduction in power production.[5] Also, the presence of different type of constraints such as noise control, investment cost, inter-turbine distance, longevity of the turbine, and visual impacts adds further complexity to the problem.[6] Apart from these, development of wind farms in the close proximity of human dwellings, natural habitats (rivers, lakes forests, etc.), or forbidden zones (where for different reasons turbines cannot be placed) also restricts its wide acceptance.[7]

Two primary ways of approaching the LO problem are (i) discretizing the given wind farm area into uniform grids and thereafter considering the grid mid or junction points as the potential turbine locations (viz. grid approach)[8–10] and (ii) using any coordinate in the given wind farm area without grid restrictions (viz. no-grid approach).[11–13] Guessing a value for the maximum number of turbines that can be accommodated inside a wind farm, an equivalent number of coordinate locations (continuous variables) are selected, and a set of binary variables (1 and 0 to signify presence and absence of turbine, respectively) is associated with each of these locations. One can finally determine the actual number (summing the binaries) and location of turbines in the layout while optimizing over these continuous and binary forms of variables, in the presence of many other constraints. One such constraint could be a prespecified inter-turbine distance, which helps to avoid wake interactions between the turbines; however, this might restrict the turbine numbers that can be placed optimally in a farm.[14] These formulations are known as mixed integer nonlinear programming problems (MINLPs) that might suffer from the combinatorial explosion with an increase in problem size (known as NP hardness). Though it might appear that the number of alternative locations available to the grid approach is significantly less than that of the no-grid approach, the number itself could be staggering for a reasonable grid size, where further increase in grid size has to face the trade-off between accuracy and execution time. On the other hand, dropping the binary variables from the formulation, that is, determination of optimum positions of a fixed number of turbines (nonlinear programming problems, NLP), makes the problem relatively easier to solve.

Following the grid approach, Mosetti et al.[8] used the binary coded single objective Genetic Algorithm (GA) to find the locations of turbines while minimizing the weighted form of cost–power as a single objective problem. These results were further improved by Grady et al.[9] with modification in the objective function and optimization parameters. Mimicking an exponential velocity decay in the wake model, Parada et al.[10] proposed the Gaussian wake model to maximize the annual energy output of a wind farm. On the other hand, using no-grid approach, where turbines can be freely placed in a farm, Wan et al. reported an improvement of ∼5–7% in power production as compared with the grid results utilizing the real coded GA[11] and Gaussian particle swarm optimization (GPSO)[12] approaches, respectively. Gu and Wang[13] utilized a systematic no-grid approach to deal with irregular shape of a wind farm, where a combination of single, multiple boundary constraint models, and the ray intersection method was proposed to accomplish the wind farm micrositing in the presence of boundary constraints. Parallely, efforts have also been spent to increase the power production out of a wind farm by adopting different mathematical techniques and by controlling the characteristics of wind generators (such as generator torque, blade pitch and tip ratio, hub height, and yaw alignment).[2,15]

However, most of these above formulations considered the LO problem with known number of turbines (NLP problem). Mittal et al.[16] reported better quality solutions adopting an iterative approach utilizing both grid and no-grid based methods. In this approach, at every iteration, evolutionary methods at first find both number and locations of turbines utilizing a grid framework, and the classical methods are used next to improve only the locations keeping the number of turbines fixed. Pookpunt and Ongsakul[17] utilized the modified binary particle swarm optimization algorithm to optimally locate the wind turbines as well as their types in a layout while aiming for maximum operating income. Furthermore, major challenges like control of noise,[8,9,18–20] presence of forbidden zones (lakes, roads, etc.),[21,22] wind state forecasting,[23] and uncertainty in the wind distribution[24]etc. were also considered to perform the LO.

In this work, the target is to solve the LO problem in an efficient manner. As opposed to previous approaches, a multiobjective optimization is studied here considering three important but conflicting objectives simultaneously (i.e., maximization of energy generation, minimization of noise propagation, and the minimization of investment cost). Instead of handling an enormously large number of candidate sets in case of the continuous formulation, a grid-based approach has been adopted here with an aim of reducing the computational cost and improving the solution quality. Representing the grid points with indices, an index-based decomposition and repair strategy (iDRS) has been proposed in this work to solve the LO problem along with a performance enhancement repair policy. Apart from this, the performance of the proposed algorithm, which is implemented within the platform of NSGA II,[25] is further improved by refreshing the matured population with certain fresh candidate solutions to avoid the premature convergence of the algorithm. After implementing the novel concepts of repair strategy and rejuvenation of solution pool with fresh candidate solutions, the proposed algorithm is applied on the realistic case with real-time wind speed and directional distribution,[17] and the effects of the presence of practical constraints such as human dwelling and irregular forbidden zone are analyzed on the optimal layouts of wind turbines inside a wind farm. The remaining part of the paper goes as follows. The calculation of wake modeling, power production, investment cost, and noise propagation is shown in Section 2 whereas multiobjective formulation of cost–power is described in the following section. The index-based approach is presented in Section 4. The application of proposed approach on representative case studies and their outcomes are shown in Section 5, and finally, Section 6 concludes the study.

2 | WAKE, POWER, AND NOISE MODELING

Because of wake interference caused among turbines in a cluster, a downwind turbine observes a different wind speed compared with the incoming free stream wind speed (u_∞) inside a wind farm. The model[2] for linear wake propagation behind a wind turbine is considered to compute the

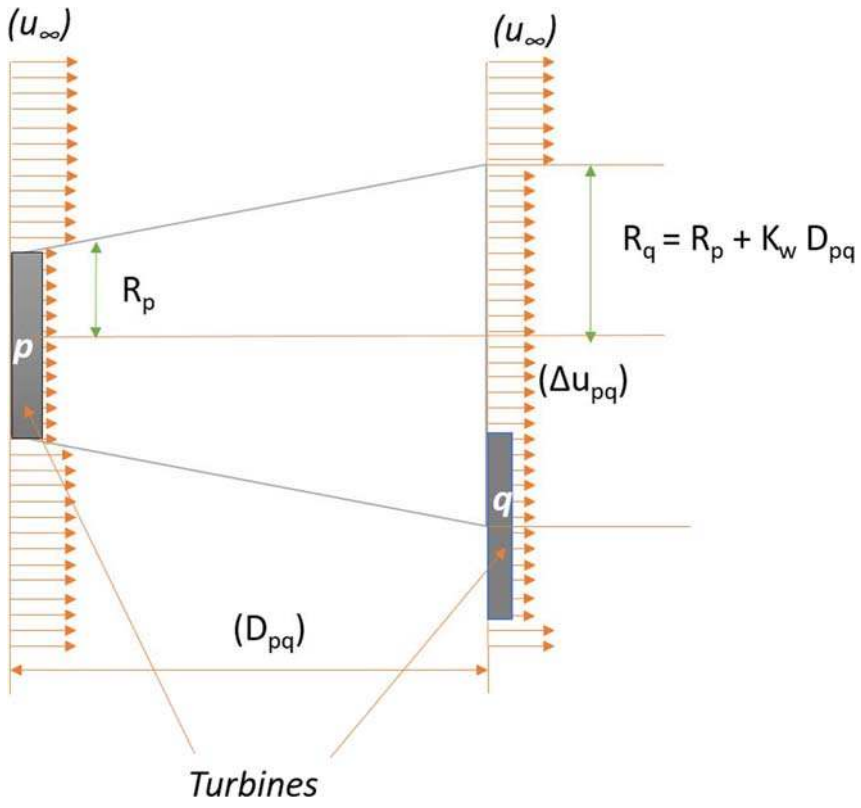

FIGURE 1 Schematic view of linear wake propagation between turbines [Colour figure can be viewed at wileyonlinelibrary.com]

reduced velocity faced by the downwind turbine (Figure 1). In this wake model, the effect of upwind turbine "p" at a distance of (D_{pq}) on the downwind turbine "q" can be represented as follows[8]:

$$\Delta u_{pq} = u_\infty \times \left[1 - \left(\frac{2 \times \alpha}{(1 + K_w \times (D_{pq}/R_p))^2}\right)\right] \tag{1}$$

Here, (Δu_{pq}) represents reduction in speed of wind experienced by a downwind turbine "q"; entrainment coefficient and downstream rotor radius are represented by K_w and R_p, respectively. According to the Betz relation, downstream rotor radius (R_p), the coefficient of thrust (C_T), rotor radius (R_t), and axial induction factor (α) can be related as follows[9]:

$$R_p = R_t \times \sqrt{\frac{1-\alpha}{1-2\times\alpha}},\ \alpha = 0.5 \times \left(1 - \sqrt{1 - C_T}\right) \tag{2}$$

And, the wake decay constant can be expressed as follows:

$$K_w = \frac{0.5}{\ln(Z_{turb}/Z_{ro})} \tag{3}$$

where Z_{turb} and Z_{ro} are the turbine hub height and surface roughness of a wind farm, respectively. In reality, the actual velocity deficit (u_{def}) at the downwind turbine is equal to the sum of the velocity deficits (Δu_{pq}, Equation 1) induced by the number of upwind wind turbines (N_{upwind}), which can be calculated using the following expression 8:

$$\left(1 - \frac{u_{def}}{u_\infty}\right)^2 = \sum_{i=1,\ i\neq q}^{N_{upwind}} \left(1 - \frac{\Delta u_{iq}}{u_\infty}\right)^2 \tag{4}$$

Moreover, the variation in wind speed (u_{var}) at different altitudes (Z_{alt}) with respect to reference values of speed (u_{ref}) and height (Z_{ref}) can be calculated using power law[17] as follows:

$$u_{var} = u_{ref} \times \left(\frac{Z_{alt}}{Z_{ref}}\right)^{(1/\ln(Z_{alt}/Z_o))} \tag{5}$$

Generally, the variants of wind speed such as cut-in (u_{cin}), cut-out (u_{cout}), rated (u_{rt}), actual deficit wind speed (u_{def}), and rated power of a turbine (P_{rt}), are used to calculate the power output (in kW) of a turbine (Pwr) using turbine power curve.[16] Moreover, the product of individual turbine power (Pwr) and the frequency distribution of occurrence of wind ($Freq_{no}$) summed over wind coming from all directions at different wind speeds for all turbines provides the total power production (P_{total}) in a wind farm (6):

$$P_{total} = \sum_{m=1}^{N_T}\left[\sum_{n=1}^{360^\circ}\sum_{o=1}^{u_{max}} Freq_{no}(\theta_n, u_o) \times Pwr_{no}(\theta_n, u_{def,o})\right] \tag{6}$$

Here, "o," "n," and "m" are the subscripts to perform discrete summation over wind speed (u), direction (θ), and number of turbines (k), respectively. N_T and u_{max} are the total number of turbines present in a wind farm and maximum value of wind speed bins, respectively. The frequency of occurrence of wind ($Freq_{no}$) at different directions and speeds is presented as a probability mass function as shown in Figure 2. The entire range of wind speed (3–25 m/s) and direction (e.g., 0–360°) is divided into different numbers of adjacent discrete bins, that is, there are "n" bins for direction (0–30°, 30–60°, etc.) and "o" bins for speed (3–4, 4–5, etc.). The frequency of occurrence of wind due to a particular combination of speed and direction bin is expressed as the ratio of wind occurrences in those bins and the total number of wind occurrences due to all bin combinations. In order to compute the individual power output of a particular turbine (say m), at first, the actual input wind speed deficit (Equation 4) is calculated at the selected turbine, which can either be influenced by no upwind turbines or N_{upwind} numbers of upwind turbines depending on the location of a turbine. Next, using the turbine power curve, provided by a turbine manufacturer, the corresponding power generated by a wind turbine is calculated. Thus, the total power generated by a selected turbine (say m) is given as the product of individual power and the frequency of occurrence of wind flow at a particular direction (n) and at a particular wind speed bins (o) in a wind farm. In a similar fashion, this exercise is performed for all the wind speeds and directions of the wind flow and summed over the total number of turbines to measure the total power production (P_{total}) in a wind farm for a specific turbine layout.

Also, the annual energy production (AEP) (in kWh) of a wind farm is given as follows:

$$AEP = 8760 \times P_{total} \tag{7}$$

For investment cost calculation, the contributions of fixed cost and variable cost are assumed to be in the ratio of 2:1 on yearly basis and can be expressed as follows[8]:

$$cost = N_T \times \left(\frac{2}{3} + \frac{1}{3} \times \exp(-0.00174 \times N_T^2)\right) \tag{8}$$

Here, noise propagation is calculated using ISO-9613-2 acoustic model.[2] As per this model, the sound pressure level (SPL), L_P, at every location of receptor is given as follows:

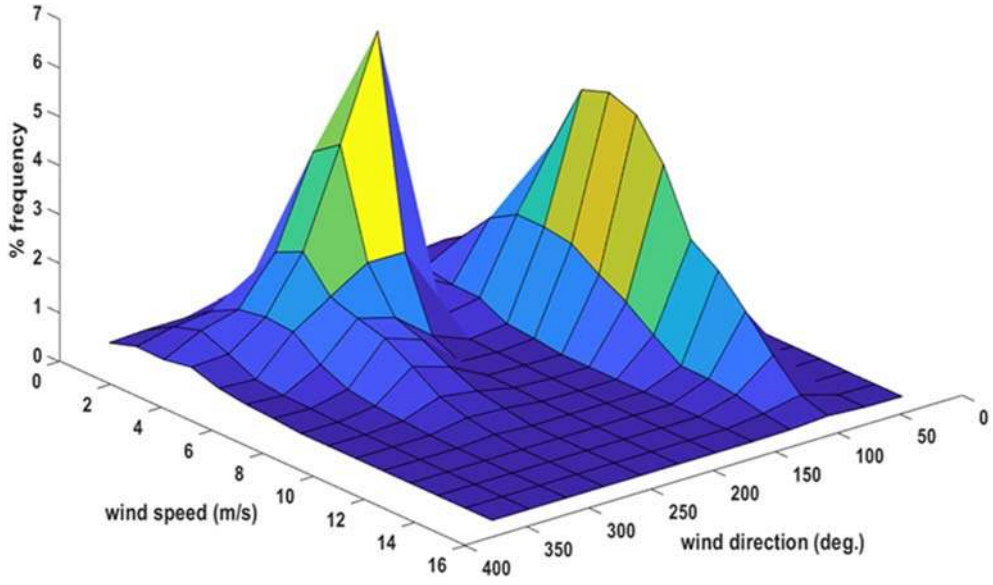

FIGURE 2 The frequency of occurrence distribution at different wind states (speed and direction) for a realistic case [Colour figure can be viewed at wileyonlinelibrary.com]

$$L_P = L_w + D_C - A_f \tag{9}$$

where f represents frequency value of each band (octave), L_w represents octave-band sound power from source (100 dBA),[2] D_C is the directivity correction for non-omni directional sound sources, and A_f is for different attenuation effects of octave band. In general, hearing risk at any specified location can be represented as (A-weighted level ($L_{P,avg}$))

$$L_{P,avg} = 10 \times \log\left(\sum_{i=1}^{N_s}\left(\sum_{j=1}^{8} 10^{0.1 \times (L_P(i,j) + A_f(j))}\right)\right) \tag{10}$$

where index "j" is for eight octave band frequencies and N_S is the number of sound sources. Considering the Euclidean distance between the sound source(s) and receptor(s), the estimated SPL can be given as follows:

$$L_P(d_{ir}) = L_w - 10 \times \log_{10}\left(2\pi d_{ir}^2\right) - \beta \times d_{ir} \tag{11}$$

where the indices "i" and "r" are for individual sound source and receptor locations, respectively; d_{ir} is the Euclidean distance between the wind turbine (sound source) and receptors (eg., a human habitat); β represents the coefficient of sound absorption (0.005 dB/m).[2] For multiple receptors, $L_{P,avg}$ is calculated separately for each sound source using (10) and (11). *Here, SPL is referred as "Noise", the human habitats inside or in the neighborhood of wind farms are assumed to be considered as noise receptors and wind turbines as sound sources, respectively.*

3 | PROBLEM FORMULATION

The problem of determination of optimal layouts while considering the impacts of presence of practical constraints inside a wind farm has been targeted here. Since it is established that there exist trade-offs between the power–cost[8] and power–noise,[18] according to the principles of multi-objective optimization (MOO),[25] power, cost, and noise are conflicting to one another, when considering all of them, simultaneously. Hence, MOO formulation simultaneously maximizing power and minimizing noise level and cost of investment can be mathematically expressed as follows:

$$\text{Objective}: \min_{(\bar{x},\bar{y},\bar{b})} \left(-P_{total}(L_{xy}),\ \text{cost}(L_{xy}),\ \text{Noise}(L_{xy})\right) \tag{12}$$

subject to

$$G_1(x_p, y_p) = D_{sp} \times D_{ro} - \sqrt{(x_p - x_q)^2 - (y_p - y_q)^2} \le 0 \forall p, q = 1, \ldots, N_T\ s.t. p \neq q \tag{13}$$

$$\text{Decision variable set}: x_p, y_p, b \tag{14}$$

Here, P_{total}, cost, and Noise are presented in Equations 6, 8, and 10, respectively; $\bar{x}, \bar{y}, \& \bar{b}$ are the continuous (location coordinates) and binary decision variables; L_{xy} is the layout with N_T number of turbines ($\forall b = 1$) and (x_p, y_p) are turbine locations for this layout; $G_1(x_p, y_p)$ is the constraint for interturbine distance (ITD) to avoid wake loss; D_{sp} is multiplier in ITD; D_{ro} is for rotor diameter. After discretizing the wind farm using certain grid resolution, the location coordinates of turbines are represented by indices $Idx(x_p, y_p)$ ($p = 1 \ldots N_T$). They replace the location coordinates and act as modified decision variables. Assuming N_{GRIDS} number of grids in the discretized farm, a decision variable set of cardinality N_L is assumed. This N_L is the number of turbines that can be accommodated in the farm. Each of N_L index variable is distinct and can assume any index in between 1 and N_{GRIDS}. The binary variable ("b") element in the set of cardinality N_L designates the absence or presence of turbines at these index locations (assuming either 0 or 1, respectively). Each index variable, which is integer in nature, is connected with a continuous coordinate in the wind farm. Since both integer (binary) and continuous form of variables are present, this formulation belongs to the category of MINLP.

Furthermore, in the realistic case studies considered, the effects of presence of practical entities such as human habitats and forbidden zone inside a wind farm are scrutinized on the optimal results. Human habitats, as explained in Section 2, can be represented by sound receptors inside a wind farm, whereas a new regulatory constraint (G_2) can be used to represent the forbidden zone. Using a single boundary ray intersection method,[13] the presence or absence of wind turbines inside a restricted zone is evaluated. In this method, wind turbine(s) are assumed

as point(s) and restricted zone as a polygon (convex or concave). At first, the intersection point(s) (Z_q) between the vertical half line drawn from the selected i^{th} wind turbine locations (x_i, y_i) (i = 1, ..., N_T) and the edge(s) (ex_q,ex_{q+1}) (q = 1, ...,total number of edges) of the restricted zone are evaluated using two-point slope formula as shown in (15):

$$z_q(x_i) = \frac{ey_{q+1} - ey_q}{ex_{q+1} - ex_q}(x_i - ex_q) + ey_q \tag{15}$$

Here, ex_q and ey_q (q = 1, ...,total number of edges) represent the x and y-coordinates of an edge of a restricted zone. By keeping the check on whether the selected turbine position point lies inside (value = 1) or outside (value = 0) the edge, the number of intersections (Δ_q) is calculated for each edge and then summed up as total number of intersections ($\lambda(x_i)$), which is given by

$$\Delta_q = \begin{cases} 1, y_i < z_q(x_i) \\ 0, otherwise \end{cases}, \ \lambda(x_i) = \sum\nolimits_{q=1} \Delta_q \tag{16}$$

Furthermore, depending on the total number of intersections, a modulo operator is applied to determine the value of intersection criteria as shown in (17). This criterion is calculated based on the even or odd nature of value for the total number of intersections; that is, if the total number of intersections is an even number, the modulo operator returns zero value as an outcome. Thus, the value of intersection criteria equals to zero means the point is lying outside the polygon. This is because the vertical half line drawn from the point outside the polygon would make an even number of intersection with all polygon edges considered together. On the other hand, the value of the intersection criteria will be 1 in case a point is lying inside the polygon (due to an odd number of intersections by vertical half line with all polygon edges considered together).[13]

$$\phi(x_i) = \begin{cases} 0, \ \mathrm{mod}(\lambda(x_i), 2) = 0 \\ 1, \ otherwise \end{cases} \tag{17}$$

This whole process is repeated for all turbines, and the constraint G_2 is calculated as shown in (18). It is to be noted that the constraint G_2 is supposed to be satisfied, when no turbine is present inside a restricted zone.

$$G_2 = \sum\nolimits_{i=1}^{N_T} \phi(x_i) / N_T \ \leq \ 0 \tag{18}$$

As an unconstrained problem is relatively easier to solve, the above constrained problem is modified as unconstrained problem using modifying parameters (M_1 and M_2) as shown in (19)–(25)[18]:

$$\sigma_1(x_r, y_r) = \frac{\sqrt{(x_r - x_s)^2 - (y_r - y_s)^2}}{D_{space} \times D_{ro}} \ \forall r, s = 1, ..., N_T \ s.t. \ r \neq s \tag{19}$$

$$\psi_{rs}(x_r, y_r) = \left\{ \begin{matrix} (\sigma_1(x_r, y_r))^2, \ \sigma_1(x_r, y_r) < 1 \\ 1, \ \text{otherwise} \end{matrix} \right\} \tag{20}$$

$$M_1 = \prod (\psi_{rs}(x_r, y_r)) \tag{21}$$

$$M_2 = \begin{cases} 1, \ G_2 \leq 0 \\ G_2, \ otherwise \end{cases} \tag{22}$$

$$P1_{total}(L_{xy}) = P_{total}(L_{xy}) \times M_1 \times M_2 \tag{23}$$

$$\text{cost1}(L_{xy}) = \text{cost}(L_{xy})/(M_1 \times M_2) \tag{24}$$

$$\text{Noise1}(L_{xy}) = \text{SPL}(L_{xy})/(M_1 \times M_2) \tag{25}$$

$$\text{ModObjective}: \min_{(\bar{x},\bar{y},\bar{b})}(-P1_{\text{total}}(L_{xy}), \text{cost1}(L_{xy}), \text{Noise1}(L_{xy})) \tag{26}$$

where $\sigma_1(x_r, y_r)$, $\psi_{rs}(x_r, y_r)$ are the normalized parameters used to convert the value of constraint G_1 (13) in the scale of 0 to 1. M_1 and M_2 are the modified parameters that are multiplied or divided to further increase, decrease, or to penalize (in case of constraint violation, i.e., $(\sigma_1(x_r, y_r) < 1$ and $G_2 > 0)$ the objective function. This modification enables lower values of power, higher values of cost, and noise in case of constraint violation, which makes infeasible solutions inferior compared to the feasible solutions in terms of objective function. This helps the optimizer to make correct (preferring feasible over infeasible solutions) choice while comparing these solutions. The reverse logic is followed when constraints are satisfied. Using these modified operators, the modified value of generated power ($P1_{\text{total}}$), the investment cost (cost1), and noise propagation (Noise1) are calculated, respectively. In this way, the modified objective function values (Mod-Objective as in equation 26) are used for the unconstrained multiobjective optimization problem. The characteristic features and data for model development and problem formulation used in this study are presented in Table 1.[16,17]

4 | METHODOLOGY

Two types of formulations that dominate the LO problem are discrete (i.e., grid-based) and continuous versions of it. In the continuous form, first a fictitious number of turbines (N_L) are assumed to be placed inside the wind farm, and the location coordinates (x and y) for these turbines are determined within the given boundary of a wind farm. As N_L is not known in the beginning and has to be determined optimally, equal number (N_L) of binary variables are associated with the location coordinates to denote presence or absence (binary variable equals 1 or 0) of turbines at those locations. In this way, the decision variable set assumes a size of $3 \times N_L$, which might be a large number even for a small value of N_L. On the other hand, in discrete grid methods, the farm is decomposed into grid points (N_{GRIDS}) of same size and each grid point considered as turbine locations in the decision variable set. Here, each location is attached with a binary variable representing their presence or absence, by 1 or 0 values, respectively. So, depending on grid resolution, length of decision variables (both the *x* and *y* location coordinates and binaries) varies. For a coarse grid resolution case (say 10×10 grids, $N_{GRIDS} = 100$), the length of decision variable might be small ($3 \times N_{GRIDS}$, in this case 300), but inferior quality solutions might surface as some other potential locations, which are not present on the grid, are not explored. The solution quality can be improved with finer grid resolution (say, 51×51 grids, $N_{GRIDS} = 2{,}601$), but the size of the decision variable set (real [x and y], binary string length) increases, and thereby, the size of the optimization problem becomes larger ($3 \times N_{GRIDS}$, in this case 7,803). This points to an increase in combinatorial complexity apart from more memory required for storage and operations for the increased decision variable set, leading to inefficient functioning of optimization algorithms. An efficient way to handle this situation is to represent each coordinate location in a grid approach by different index numbers and then consider only few of them, not all, in the decision variable set at a time. To start with, this index selection can be done randomly. In this way, a relatively small number of location coordinates (or decision variable size), N_{Idx} ($\leq N_L$ or $< << N_{GRIDS}$) can be considered, where N_{Idx} number of indices and binary variables each can be regarded as the reduced set of decision variables As the proposed problem

TABLE 1 Wind farm, wind turbine, and wake model, constraints specifications for case studies

Cases	Test	Realistic
Wind farm		
Area (in m^2)	2000×2000	2000×2000
Roughness (Z_{ro})	0.3	0.3
Wind turbine and wake model		
Power (P_{rt}, in kW)	629.1	850
Height (Z_{turb} in m)	60	60
Diameter (D_{ro} in m)	40	52
Power curve (in kW)	$0.3u^3$	[16]
Thrust coefficient (C_T)	0.88	[16]
Constraints		
ITD multiplier (D_{sp})	5	5

formulation (26) is multiobjective in nature, it has been solved using a modified version of NSGA II[25] that uses the concept of index-binary forms of decision variables and repair strategy (henceforth called as iDRS NSGA II). This algorithm has the following components:

4.1 | Initialize the population

The given area of farm is first discretized into square grids of same size, where distinct binary and index variables are connected with each point on grid. In the chromosomal representation of GA, this can be presented by placing N_{Idx} length of indices and N_{Idx} length of binaries side by side. In this way, the string length of such a chromosome is $2\times N_{Idx}$. This N_{Idx} value is generally kept less than N_{GRIDS} signifying it as the maximum accommodating turbines. The values of indices in the index array are chosen from a set of, for example, 10×10 ($N_{GRIDS} = 100$) indices (within $1 \le N_{Idx} \le N_{GRIDS}$) without repetition to start with (can be anything different from 10×10). Binary locations can assume 1 or 0 signifying the presence or absence of turbines at these indices (locations). Every iteration, named as generation, is composed of population (N_{POP}) of such candidate solutions (or chromosomes), and such population of index-binary solutions are generated randomly in the beginning.

4.2 | Fitness computation and GA operators

By considering only the indices with binary value 1 in a chromosome (as turbines only exist for those locations), the modified objective function of N_{POP} such chromosomes are calculated using Equation 26. Next, the variation operators such as cross-over and mutation are operated on the population to generate a set of new N_{POP} offsprings. On real variables, variation operators, namely, simulated binary crossover and polynomial mutation, have been used whereas on binary variables, single point crossover and binary mutation have been applied as variation operators, respectively.[25] Combining N_{POP} parents with N_{POP} offsprings (elitist strategy), the combined pool of population ($2\times N_{POP}$) went through the steps of nondominated sorting and crowding distance-based Elitism approach to provide the best set of N_{POP} nondominated chromosomes, which can be used as a starting population for next generation.[25] Since different objective function values are compared among different chromosomes while performing nondominated sorting, they are generally expressed with the same notion of optimization, for example, maximization or minimization. Following this, all objectives are expressed here with the notion of minimization. Maximization of power production is first converted into the minimization form by considering the −ve value of Power, that is, Min (− Power) as given in Equations 12 and 26, respectively, thereby representing all objective functions by minimization type. In this way, the logic written for nondominated sorting considering all minimization type of objectives is going to be applicable for this case. In case of negative objective function, more negative the objective function becomes, better it is considered while performing nondominating sorting. This completes one generation of NSGA II, and it continues till the total number of generations, Gen_{max}, specified in the beginning, is reached. Inquisitive readers can refer literature[25] for more details about NSGA II.

4.3 | Novel repair strategy

Using the aforementioned variation operators, the speed of convergence is observed to be slow for the targeted micrositing problem. Moreover, the specific challenge is to select a suitable length of N_{Idx} indices out of bigger set of N_{GRIDS} (as $N_{Idx} << N_{GRIDS}$), so that better solution can be found quickly. To accelerate the convergence rate of an algorithm and to further enhance the potential of variation operators, a novel repair strategy has been proposed in this study. Starting with the coarse resolution of grid, the steps of initialization, function evaluation, variation continue as usual. Next, based on the predescribed repair probability (P_{repair}), chromosome(s) are selected (Figure 3A) from the new population for repair with a target of improving their feasibility (if originally infeasible) and objective function values by repairing both index and binary variables. To perform repair on indices, first the index that is most crowded (CI_{Index}) (i.e., the index which is surrounded by many nearby indices) has been identified (Figure 3B). Here, CI_{Index} is calculated using the corresponding location coordinates (x and y) values of all the indices in the selected chromosome (with binary value 1) as shown in Equations 27 and 28:

$$\mathrm{Dist}_{\mathrm{index}}(i) = \min\left(\sqrt{(x_i - x_j)^2 - (y_i - y_j)^2}\right) \ \forall i,j = 1,\ldots,N_T \ s.t. i \neq j \tag{27}$$

$$\mathrm{CI}_{\mathrm{index}} = \mathrm{argmin}(\mathrm{Dist}_{\mathrm{index}}(i)), i = 1,\ldots,N_T \tag{28}$$

Here, $\mathrm{Dist}_{\mathrm{index}}(m)$ represents the minimum distance value among all the combinations of index "m" and all other indices "n." After identifying the most crowded index (CI_{Index}) to be repaired, a new index is searched for replacement inside a circle of radius SR_{space} surrounding the CI_{Index} (Figure 3C). Here, only those indices that satisfy ITD (13) are selected as possible candidates. Among these possible candidates, a new index will

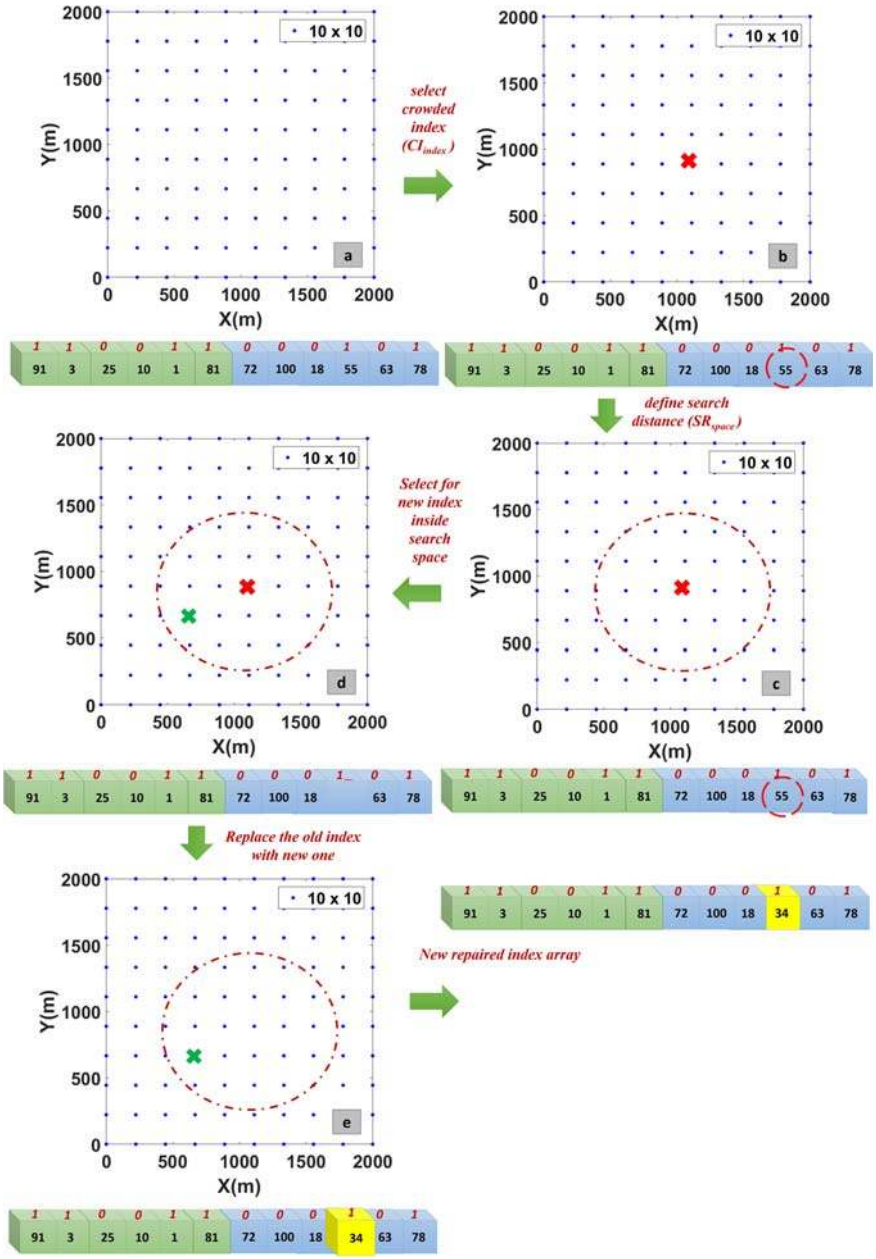

FIGURE 3 Step-by-step procedure of novel index repair strategy [Colour figure can be viewed at wileyonlinelibrary.com]

be chosen, which provide better feasibility and/or objective values while replacing the old index (Figure 3D,E). Here, replacement only happens if improvement in objective function values and/or feasibility is observed.

On the other hand, in binary repair, the chromosome that is having minimum number of 0's can be selected, and the aim is to convert those 0's into 1's (one at a time) to push more turbines in the farm. Replacement of chromosome happens only if a solution with improvement solution quality is found.

4.4 | Rejuvenation with fresh seeding

Because of the involvement of huge number of binaries, MINLPs have a chance to converge at local optimum prematurely unless a significant amount of exploration is provided during the evolution of the algorithm. Initializing the population with randomly generated fresh index-binary candidate solutions after certain fixed interval of generations (interval 1) can act as remedial measure.

After executing the aforementioned steps, the set of Pareto solutions[25] is generated (the set is known as Pareto front or PO front). Here, every solution on PO front corresponds to the combination of index-binary variables along with the alternative power-cost-noise values. Index values corresponding to binary variable value 1 are considered as the optimal turbine positions with sum of all binaries giving the optimum number of turbines in a farm. A machine with Intel® Xeon® 128-GB RAM dual processor is used for all reported simulations.

5 | RESULTS AND DISCUSSIONS

The effect of simultaneous energy generation, noise propagation, and investment cost is studied over the realistic case study based on a real-time wind speed distribution data adopted from literature[17] to see their effects on micrositing. Figure 2 shows the three-dimensional distribution of frequency, speed, and direction inside a wind farm. The MOO problem is solved using the proposed iDRS approach and the effects of presence of practical constraint such as human habitats and irregular-shaped forbidden zone, noise receptors are analyzed on the layouts for case studies. First, the suggested methodology is corroborated with a rigorously explored case study in literature[8,9,11,16] followed by another realistic case. In the former case, wind is assumed to flow at 12 m/s in a farm having an area of 2000×2000 m^2. Table 1 shows the specifications and characteristics of wind turbines, wind farm, and wake model used in this case study. The given wind farm is first mapped with 20×20 grids thereby creating 400 (N_{GRIDS}) possible locations. Assuming N_{Idx} as 100 ($<< N_{GRIDS}$), 100 distinct indices are selected randomly from the set of 400 possibilities and 100 bits of binary variables (0 or 1) associated with them. This represents a chromosome in the population as explained in the initializing population step (Section 4). With this kind of chromosome setup, an MOO problem is solved (19–26). To maintain the integrity, there are no human habitats and irregular forbidden zones considered inside a wind farm for this case; that is, the constraint G_2 (Equation 18) is not considered, and the value of M_2 (Equation 22) is considered as 1. Also, with no receptors and human habitats in place, the SPL (Equations 10 and 25) is not included while solving the MOO problem (19–26). The optimization problem of maximization of energy and minimization of cost is solved using iDRS NSGA-II, details of which are described in Table 2. The negligible amount of change in objective function values in between two immediate fresh seed cycles is set as a termination criterion, and it is achieved in six such cycles. This leads to evolution of PO front, where every set member is an optimal layout (numbers and locations) along with the conflicting values of power and cost. As the convention followed by earlier works[8,9] to report the performance of algorithm corresponding to a solution with minimum ratio of cost versus power (MCP) ($\$kW^{-1}$), a solution with MCP is selected from PO set for comparison. It is evident that the proposed approach provides better solution with 2.5–14.8% increase in cost–power ratio in contrast with other works reported (Table 3). Furthermore, the proposed approach (iDRS) with different repair probabilities is compared with the approach of without-repair as shown in Table 4. Decision on the value of repair probability was difficult to arrive at as on both higher and lower values of repair probability compared with 0.5 gave encouraging results. However, a very high value of repair probability was not found to be encouraging. Here, also a solution with MCP is selected from the PO set for the comparison. It can be seen that the P_{repair} of 0.5 value provides an improvement of $\sim$2% in power production as compared with the case of without repair method. The value of repair probability for other studies is kept fixed at 0.5 in this work though any other values of repair probability could have been used. Therefore, the enhanced performance of the proposed iDRS approach is recorded here. The proposed approach is next applied to a realistic case to study the impact of practical constraints on the optimal layout of turbines.

TABLE 2 Specifications of the proposed iDRS approach for the case studies

iDRS specifications	
Algorithm	**Elitistm**
Population (N_{POP})	200
Total generations (GEN_{max})	21,000
X-over probability (P_{cross})	0.95
X-over type	SBX and uniform X-over
Mutation probability (P_{mut})	0.05
Mutation type	Polynomial
Array length (N_{Idx})	100
Fresh-seed (interval 1)	3,000
Repair probability (P_{repair})	0.5

TABLE 3 Comparison between the proposed iDRS approach and the previous reported works for test case

S. No.	References	Total turbines (N_T)	Power (kW, 10^4)	Cost/P_{total} ($\$kW^{-1}$, 10^{-3})	% improvement in $\$kW^{-1}$
1	Mosetti et al.[8]	26	1.2352	1.6197	14.78051
2	Wan et al.[12]	30	1.5552	1.4158	2.507416
3	Mittal et al.[16]	44	2.074254	1.4386	4.052551
4	Yin et al.[24]	30	1.5091	1.4637	5.697889
5	Parada et al.[10]	30	1.5302	1.4390	4.079222
7	**Proposed SDwR**	41	2.033358	**1.3803**	---

TABLE 4 Comparison between the proposed iDRS approach and the without repair method for different repair probabilities (P_{repair})

S. No.	Repair probability (P_{repair})	Total turbines (N_T)	Power (kW)	Cost/P_{total} ($kW^{-1})	% improvement in power value
1	0.2	44	21581.38	0.0013826	8.36
2	0.4	53	25088.46	0.0014137	25.97
3	**0.5**	**41**	**20333.58**	**0.0013803**	**2.099**
4	0.6	49	23526.91	0.0013991	18.13
5	0.8	13	6739.19	0.0017652	−66.16

TABLE 5 Convergence criterion for realistic case using iDRS approach

Individual problems	Fresh-seed generations
	Realistic case
Without receptors	5
With receptors @ boundary	7
With receptors @ boundary + human habitats	7
With receptors @ boundary + human habitats + forbidden zone	7

Note: Better results are obtained at early fresh seeds; in order to satisfy the termination criterion, the more fresh seed cycles are executed.

A real-life Huasai wind farm site with the practical wind speed data collected over a year (multidirectional multispeed wind flow) is considered here.[17] The details on the wind data and algorithmic parameters are described in Tables 1 and 2, respectively. The given farm is divided into 49×49 grids thereby creating 2,401 possibilities (N_{GRIDS}) for wind turbines to be placed. However, at every 400 m, sound receptors are placed along the boundary. The practical constraints such as human habitats and irregular forbidden zone are introduced inside a wind farm to study their impacts. Assuming $N_{Idx} = 100 << N_{GRIDS}$, 100 random indices from a set of 2,401 index members are selected, and 100 bits of binary variables are associated with them for each chromosome. An MOO problem is solved using (19–26), and optimal layout is found using proposed iDRS approach. To study the impact of practical constraints, three different instances of the problem are solved. The termination criterion of negligible amount of change in objective function values for two fresh seeds is shown in Table 5 for each problem. Following are the salient observations for each problem:

- The *first problem* is solved with only noise receptors placed on the boundary. The total number of receptors in this case is 20. As there is no restricted area (human habitats and forbidden zone) inside the wind farm in this case, constraint G_2 (18) is not considered, or the modified operator M_2 (22) is considered as 1 while performing the multiobjective optimization. The termination criterion is met in 7 cycles of fresh-seed generations (Table 5). As a result, the three-dimensional PO is obtained (Figure 4A), where each point on the PO front corresponds to the different number of turbines and their optimum locations along with triobjective trade-off values. As each point on the Pareto surface has different noise, energy, and cost values, every PO point provides a different turbine layout, and the entire Pareto set can provide a plethora of alternatives to a decision maker, where each solution can be selected wisely based on the available higher level information. In this work, we have adopted fixed noise-minimum cost-energy ratio strategy (FN-MCE) to select a layout of turbines out of several alternatives as shown in Figure 4B. In this method, first a particular noise value is chosen (say ≤50 dBA). Next, for all PO solutions within this noise limit, one with minimum cost-energy ratio ($\$kW^{-1}$) is selected. In this way, for different noise level values (60, 50, 45, and 40 dBA), different layouts of best points (FN-MCE method) can be obtained (Figure 4B). Table 6 shows the generated power, cost, noise, and number of turbines of each such best point at different noise levels. It has been noted, turbines are located towards the center of firm sacrificing the cost and energy objectives, where less noise level is observed due to the presence of noise receptors at boundary. Also the maximum energy generated in this case (5777.83 kW) is compared with the case where receptors are not present at all (i.e., only energy maximization and cost minimization). Using iDRS with same parameters, a percentage reduction of 4.8% in generated power can be observed because of the presence of receptors. *The above observations reflect the importance of noise and its effects on wind farm power production while performing the layout optimization.*
- In the *second problem*, the human habitat has been introduced inside a wind farm additionally (with noise receptors at boundary), which can be handled by placing additional receptors at the location (say two numbers). In this case also, M_2 (22) assumes a value of 1 while performing the multiobjective optimization (19–26) in the absence of the constraint G_2 (18) for irregular boundaries. The total number of receptors is 22. The final Pareto front surface after executing iDRS approach for seven fresh seeds (Table 5) is depicted in Figure 4C. The different turbine layouts obtained for different noise levels (60, 50, 45, and 40 dBA) using FN-MCE method are shown in Figure 4D. More the restrictions, lesser the energy production. A reduction of 32.5% in energy value and 0.5% increment in the noise propagation (as turbines are located close to receptors at boundary and away from human habitats) can be observed in the presence of human habitats as compared to the first problem.

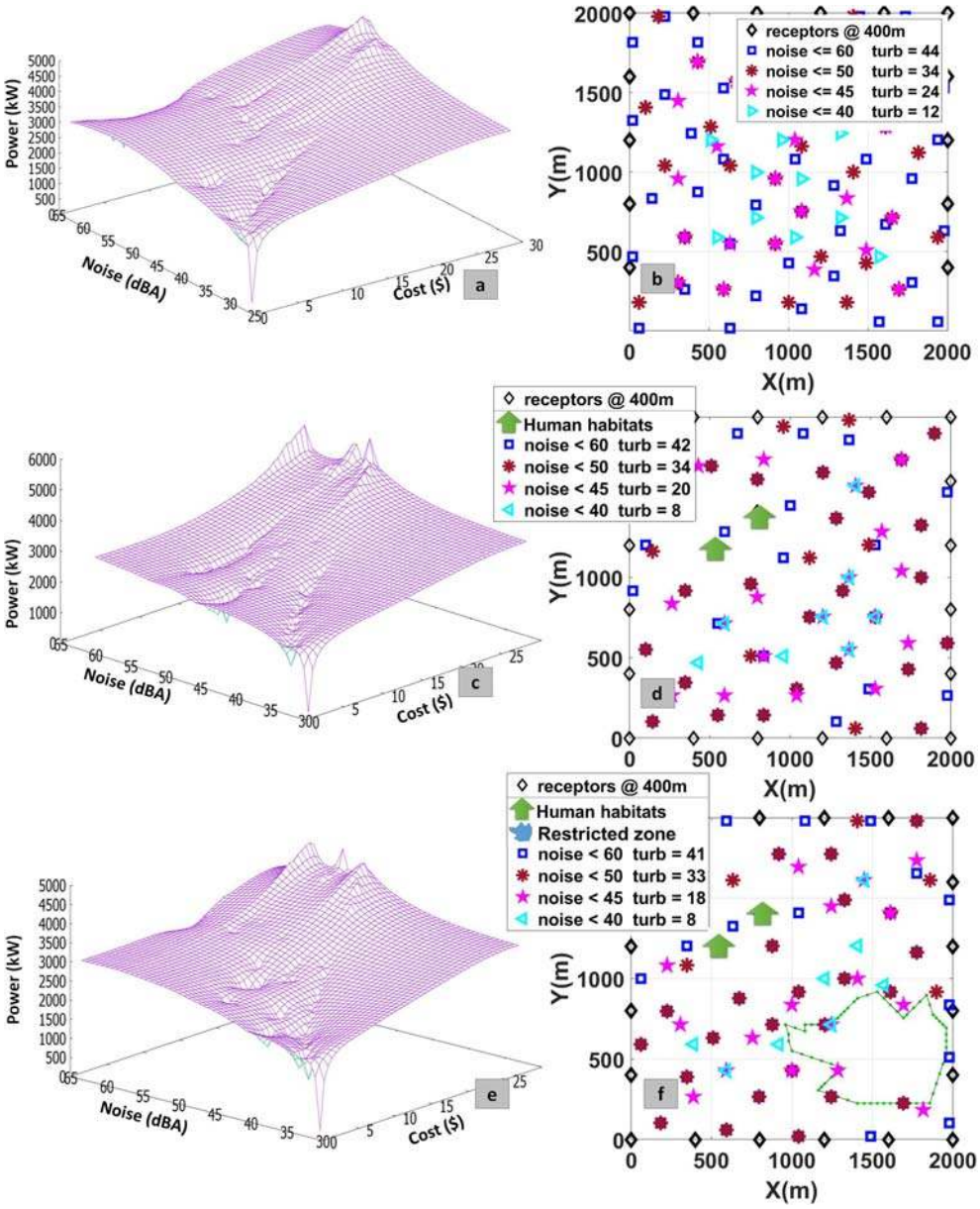

FIGURE 4 For realistic case, (A) 3D Pareto surface plot between energy-noise-cost objective functions and (B) different turbine layouts with limits on noise levels for the *first problem*; (C) energy-noise-cost 3D Pareto surface plot and (D) different turbine layouts with limits on noise levels (black square represents the human habitats [green hut shaped markers] considered as two receptors) for the *second problem*; (E) 3D Pareto surface among the objective functions and (F) different turbine layouts with limits on noise levels (green hut-shaped markers and irregular shape [blue-filled marker] represent the human habitats and forbidden zone, respectively) for the *third problem* [Colour figure can be viewed at wileyonlinelibrary.com]

Moreover, a trend of reduced energy generation and increased noise propagation and investment cost values for all the best points corresponding to each noise level as compared with the first problem can be observed (see Table 6). *This shows the change in the wind farm power production, investment cost, noise propagation, and the optimum numbers and positions of wind turbines with respect to the placement of noise receptors (or human habitats) inside or at the boundary of a wind farm.*

- In the *third problem*, more complexity is introduced by adding an irregular shaped restricted zone in the wind farm. The number of receptors remains the same as the second problem, that is, 22. Finally, a PO front is obtained after 7 fresh seeds as shown in Figure 4E. Figure 4F shows the optimal layout of turbines obtained using FN-MCE method at different noise levels. In the presence of irregular restricted zone, human habitats, and the receptors at the boundary, the overall reduction of ∼33% in energy generation as compared with the first problem, and ∼9% as compared with the second problem has been observed. Also, the increment of ∼5% and ∼7% in noise propagation can be seen as compared with the first and the second problem, respectively. Table 6 depicts the reduced energy generation, noise propagation, the investment cost, and number of turbines values for the best points at each different noise level for this case as compared with the first and second problem. It can also be seen as the number of restrictions in a wind farm increases, the optimal layout (numbers and locations) of turbines gets affected as shown in Figure 4B,D,F. For noise level < 45, number of turbines changes from 24 (in first problem) to 20 (in the second problem) and 18 (in the third problem) along with their positions. *It is, therefore, essential for a wind farm designer to consider every practical constraint with high priority while developing a wind farm.*

TABLE 6 The energy generation, noise propagation, and investment cost values at different noise levels for each individual problem solved for realistic case

	Best point				
Noise levels (dBA)	Power (kW)	Noise (dBA)	Cost ($)	Cost/P_{total} ($\$kW^{-1}$)	Number of turbines (N_T)
First problem: with receptors @ boundary					
Noise <60	5777.83	56.47	29.84	0.0051645	44
Noise <50	4453.93	49.33	24.18	0.0054298	34
Noise <45	3132.61	44.91	18.94	0.0060451	24
Noise <40	1568.31	39.61	11.11	0.0070863	12
Second problem: with receptors @ boundary + human habitats					
Noise <60	5512.01	55.16	28.65	0.0051980	42
Noise <50	4463.63	50.00	24.18	0.0054180	34
Noise <45	2629.75	44.87	16.66	0.0063343	20
Noise <40	1057.77	39.84	7.72	0.0072974	8
Third problem: with receptors @ boundary + human habitats + forbidden zone					
Noise <60	5397.88	59.54	28.07	0.0051998	41
Noise <50	4331.14	49.85	23.65	0.0054615	33
Noise <45	2367.17	44.76	15.41	0.0065118	18
Noise <40	1049.79	39.82	7.72	0.0073529	8

6 | CONCLUSION

A multiobjective optimization study with an aim of maximization of energy, minimization of cost, and noise propagation has been performed to determine the optimum layout in a wind farm in presence of practical constraints such as human dwellings, restricted zones, etc. An index-based decomposition and repair strategy (iDRS) using the concept of index representation of grids implemented on the binary-real coded NSGA II platform has been proposed to solve the problem. Index variables are used to represent locations of turbines, and binary variables are used to identify their presence/absence. The performance of the proposed algorithm is further enhanced by bringing diversity in the converged population with fresh seeding. A significant improvement of 2.5–14.8% by the proposed approach in ratio of cost and power ($\$kW^{-1}$) has been identified in contrast with works reported. Overall reduction of 32.5% and 33% in energy generation and increment of 0.5% and 5.4% in noise propagation can be observed owing to the presence of human dwellings and forbidden zone (with human dwellings) respectively, as compared with the case where they were not present. The set of PO solutions allows decision maker to choose among various competing layouts based on permissible noise levels, cost obligations, and the extent of harnessed energy.

ACKNOWLEDGEMENT

Authors like to acknowledge the support provided by the SPARC project (SPARC/2018-2019/P1084/SL) funded by the Ministry of Human Resources Development (MHRD), Government of India, for this work.

ORCID

Kishalay Mitra https://orcid.org/0000-0001-5660-6878

REFERENCES

1. Abdalrahman G, Melek W, Lien FS. Pitch angle control for a small-scale Darrieus vertical axis wind turbine with straight blades (H-type VAWT). *Renew Energy*. 2017;114:1353-1362.
2. Herbert-Acero J, Probst O, Réthoré PE, Larsen G, Castillo-Villar K. A review of methodological approaches for the design and optimization of wind farms. *Energies*. 2014;7(11):6930-7016.
3. Kumar R, Raahemifar K, Fung AS. A critical review of vertical axis wind turbines for urban applications. *Renew Sustain Energy Rev*. 2018;89:281-291.
4. Gloabal wind report. 2017. Available: http://gwec.net/publications/global%2010wind%2010report%20102/ [Accessed: January - 2019].
5. Zergane S, Smaili A, Masson C. Optimization of wind turbine placement in a wind farm using a new pseudo-random number generation method. *Renew Energy*. 2018;125:166-171.

6. Sorkhabi SY, Romero DA, Beck JC, Amon CH. Constrained multi-objective wind farm layout optimization: novel constraint handling approach based on constraint programming. *Renew Energy*. 2018;126:341-353.
7. Sorkhabi SY, Romero DA, Yan GK, et al. The impact of land use constraints in multi-objective energy-noise wind farm layout optimization. *Renew Energy*. 2016;85:359-370.
8. Mosetti GP, Poloni C, Diviacco B. Optimization of wind turbine positioning in large windfarms by means of a genetic algorithm. *J Wind Engin and Indust Aerodyn*. 1994;51(1):105-116.
9. Grady SA, Hussaini MY, Abdullah MM. Placement of wind turbines using genetic algorithms. *Renew Energy*. 2005;30(2):259-270.
10. Parada L, Herrera C, Flores P, Parada V. Wind farm layout optimization using a Gaussian-based wake model. *Renew Energy*. 2017;107:531-541.
11. Wan C, Wang J, Yang G, Zhang X. Optimal siting of wind turbines using real-coded genetic algorithms. *InProceedings Europ Wind Energy Asso Confer and Exhibi*. 2009 Mar.1–6.
12. Wan C, Wang J, Yang G, Gu H, Zhang X. Wind farm micro-siting by Gaussian particle swarm optimization with local search strategy. *Renew Energy*. 2012;48:276-286.
13. Gu H, Wang J. Irregular-shape wind farm micro-siting optimization. *Energy*. 2013;57:535-544.
14. Hou P, Hu W, Soltani M, Chen C, Chen Z. Combined optimization for offshore wind turbine micro-siting. *Appl Energy*. 2017;189:271-282.
15. van Dijk MT, van Wingerden JW, Ashuri T, Li Y. Wind farm multi-objective wake redirection for optimizing power production and loads. *Energy*. 2017;121:561-569.
16. Mittal P, Kulkarni K, Mitra K. A novel hybrid optimization methodology to optimize the total number and placement of wind turbines. *Renew Energy*. 2016;86:133-147.
17. Pookpunt S, Ongsakul W. Design of optimal wind farm configuration using a binary particle swarm optimization at Huasai district, Southern Thailand. *Energ Conver Manage*. 2016;108:160-180.
18. Mittal P, Mitra K, Kulkarni K. Optimizing the number and locations of turbines in a wind farm addressing energy-noise trade-off: a hybrid approach. *Energ Conver Manage*. 2017;132:147-160.
19. Sedaghatizadeh N, Arjomandi M, Cazzolato B, Kelso R. Wind farm noises: mechanisms and evidence for their dependency on wind direction. *Renew Energy*. 2017;109:311-322.
20. Arnold B, Lutz T, Krämer E. Design of a boundary-layer suction system for turbulent trailing-edge noise reduction of wind turbines. *Renew Energy*. 2018;123:249-262.
21. Afanasyeva S, Saari J, Pyrhönen O, Partanen J. Cuckoo search for wind farm optimization with auxiliary infrastructure. *Wind Energy*. 2018;21(10):855-875.
22. Shakoor R, Hassan MY, Raheem A, Rasheed N. Wind farm layout optimization using area dimensions and definite point selection techniques. *Renew Energy*. 2016;88:154-163.
23. Mughal MO, Lynch M, Yu F, Sutton J. Forecasting and verification of winds in an east African complex terrain using coupled mesoscale-and micro-scale models. *sJ Wind Engin and Indust Aerodyn*. 2018;176:13-20.
24. Yin PY, Wu TH, Hsu PY. Risk management of wind farm micro-siting using an enhanced genetic algorithm with simulation optimization. *Renew Energy*. 2017;107:508-521.
25. Kalyanmoy D. *Multi objective optimization using evolutionary algorithms*. John Wiley and Sons; 2001 Jun 27.

How to cite this article: Mittal P, Mitra K. Micrositing under practical constraints addressing the energy-noise-cost trade-off. *Wind Energy*. 2020;1–14. https://doi.org/10.1002/we.2525